



CHALMERS
UNIVERSITY OF TECHNOLOGY

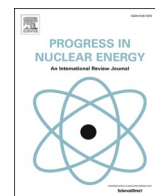
A simple model of prompt neutron leakage self-multiplication for use in nuclear materials assay

Downloaded from: <https://research.chalmers.se>, 2025-02-23 04:16 UTC

Citation for the original published paper (version of record):

Croft, S., Favalli, A., Joyce, M. et al (2025). A simple model of prompt neutron leakage self-multiplication for use in nuclear materials assay. *Progress in Nuclear Energy*, 180. <http://dx.doi.org/10.1016/j.pnucene.2025.105606>

N.B. When citing this work, cite the original published paper.



A simple model of prompt neutron leakage self-multiplication for use in nuclear materials assay

Stephen Croft^{a,*}, Andrea Favalli^b, Malcolm Joyce^a, Imre Pázsit^c, Melissa Styth^a

^a Lancaster University, Bailrigg, Lancaster, LA1 4YW, UK

^b European Commission, Joint Research Centre (JRC), Ispra, Italy

^c Chalmers University of Technology, Göteborg, Sweden

ARTICLE INFO

Keywords:

Point-model
Neutron assay
Leakage self-multiplication
Mean chord length

ABSTRACT

When assaying special nuclear materials using the passive neutron multiplicity counting method, due account must be taken of prompt neutron leakage self-multiplication in interpreting the various counting rates observed. Most often, in practical work, it is treated as an unknown model parameter to be determined from the experimental data. However, in a learning environment and when planning experiments, it is useful to have a straightforward means to estimate the leakage self-multiplication of a measurement item. In the present work, we develop a simple, hybrid, one energy-group, point-like source model for leakage self-multiplication, implemented with interaction probabilities calculated based on spherical and cylindrical bodies. We use published criticality tables to demonstrate the procedure. We show how the prompt neutron leakage self-multiplication may be estimated rudimentarily, including the effects of neutron scattering within the item. This treatment has considerable pedagogic value because it completes, in a similar conceptual framework, the physical point-model picture commonly used to interpret such neutron correlation counting-based measurements. It provides a straightforward quantitative physics-informed structure for making a forward prediction of the leakage self-multiplication factor of a compact non-reentrant measurement item, which otherwise is introduced as an unknown model parameter to be estimated only from experimental data with no guidance on how the value can be estimated *a priori*. The numerical scheme has been developed with weakly multiplying objects in mind because they are typical of the kind of items measured by thermal-neutron well-counters for nuclear safeguards accountancy and nonproliferation verification purposes. Another potential use is for the assay of measurement items of known geometry and composition where the prompt neutron self-leakage multiplication can be estimated using the simple model developed, thereby allowing the (α, n) production rate to be treated as the unknown in the practical solution (or inversion) of the usual point-model coincidence equations.

1. Introduction

Passive Neutron Coincidence Counting (PNCC) and Passive Neutron Multiplicity Counting (PNMC) are standard techniques for the non-destructive assay (NDA) of spontaneously fissioning nuclear materials. Classified as time correlation analysis methods, they are both widely used for the quantification of Pu in containerized nuclear waste as well as in nuclear safeguards applications for inventory verification, material accountancy, and control (Böhnel, 1978, 1985; Ensslin et al., 1998). The number of neutrons and the strength of the autocorrelated neutron pulse-train emerging from an item per unit mass of fissioning material present, depend on the prompt neutron leakage self-multiplication

factor. The traditional way in which this is taken into account is to use expressions for the observable total (singles) and correlated counting rates (doubles and triples when multiplicity shift-register logic is applied (Croft et al., 2012a; Croft et al., 2012b; Henzlova et al., 2012)) in terms of the properties of the measurement item and the properties of the neutron detector. The expressions are developed from consideration of the fluctuation in the neutron population emerging from a point-like source (Croft et al., 2012a; Pázsit et al., 2009; Favalli et al., 2015). Usually, the neutron capture process is considered unimportant, and the point-model expressions are developed by characterizing the measurement item solely in terms of the probability that a neutron will induce fission. The idea of a point-like source formalizes, within the

* Corresponding author.

E-mail address: s.croft@lancaster.ac.uk (S. Croft).

<https://doi.org/10.1016/j.pnucene.2025.105606>

Received 10 May 2024; Received in revised form 8 November 2024; Accepted 1 January 2025

Available online 17 January 2025

0149-1970/© 2025 The Authors. Published by Elsevier Ltd. This is an open access article under the CC BY-NC-ND license (<http://creativecommons.org/licenses/by-nc-nd/4.0/>).

mathematical description, that the interaction probabilities have no spatial dependence. This is a considerable simplification, but it allows the key functional dependencies of the various count rates to be identified in an analytically tractable and readily applicable way (Pázsit et al., 2009) and some of the inherent deficiency can be overcome through the use of empirical ‘effective’ model parameters to be estimated by calibration using reference items that are representative of the items to be measured. On the other hand, the idea of point-like items is an oxymoron in the sense that a point-source has no mass and so the point-source model, as currently formulated in the point-model framework does not of itself provide a means to estimate the fission probability for items of known configuration and fissionable material content. From a pragmatic perspective, this is not a bar to the empirical application of the point-source model to interpret the observed rates by inversion of the point-model equations because the effective prompt neutron leakage self-multiplication factor is usually treated as one of the unknown item-specific model parameters to be determined from the measurement of the item as presented. But, from a pedagogic perspective, it is unsatisfying not to have a means to make forward (predictive) calculations within the spirit and framework of the same simple and intuitive physical model. Additionally, it does not offer a simple way to enable the leakage self-multiplication to be treated as a known parameter. This is potentially of interest in the measurement of items using conventional coincidence counting where only two rates (Totals and Reals) are obtained. With only two measured quantities the measurement can only be used to estimate two unknowns. The effective ^{240}Pu mass (used to quantify the spontaneous fission rate) is one of the unknowns and for pure oxide materials (PuO_2 being the common form used to store separated Pu) the leakage self-multiplication is usually taken as the second because the (α, n) -to-spontaneous fission neutron production rate ratio can be estimated by calculation given the isotopic composition of the oxide. However, for chemically impure oxides such a calculation is no longer possible. Therefore, there may be case where it is advantageous to treat the (α, n) -to-(SF, n) ratio as unknown which requires a way to estimate the leakage self-multiplication from the known physical details of the item.

The motivation of the present work is, therefore, to document for the first time a simple hybrid model in which the interaction probabilities to be used in the point-model expressions commonly used for data interpretation are computed using un-collided escape probabilities for finite homogeneous bodies. Our approach to the problem is closely related to the way in which the fast fission effect in lumps of nuclear fuel in a thermal nuclear reactor can be estimated (Castle et al., 1943). The fast fission effect in nuclear fuel is expertly outlined in the text by Weinberg and Wigner (1958) and also introduced in several other well-known reactor physics books - usually in the context of the familiar four- or six-factor formulae for the so-called pile reproduction factor k (Littler and Raffle, 1957; Huges, 1953). In addition, in the Appendix, we complement the treatment given in the main body of the paper with a derivation of the prompt neutron leakage self-multiplication via master equations for the interaction probabilities, which also alludes to the derivation of the fast fission factor through master equations (Pál and Pázsit, 2009). Like this nuclear fuel problem, the items we are especially concerned with here have characteristic dimensions comparable to or less than fission neutrons’ mean free path (mfp). For this reason, we do not attempt an analysis based on diffusion theory, which is inappropriate for ‘optically thin’ bodies, but instead apply the statistical methods of a much-simplified random walk. Although this kind of problem is consequently well suited to Monte Carlo simulation of the full transport problem (Cashwell and Everett, 1959), we pursue the first-order analytical approach here because it is in the spirit of the point-source neutron balance equations which underlay the current theory and practice of applied time correlation neutron counting. The analytical results developed provide a long-needed self-contained picture within an analytical and readily accessible framework. Additionally, the treatment serves to demonstrate the importance of the

scattering cross-section in relation to the cross-section for the fission process. It also illustrates how to incorporate capture into the traditional point-model equations when one wants to look systematically at these effects across a range of different fissioning materials, such as relative isotopic compositions and chemical forms, and so forth. Our aim is to create a simple yet useful model to aid understanding and which is also useful as a guide and analysis tool. For instance, it raises in a very natural way the question of whether adding a pure scattering material to a multiplying item can give the impression of a larger fissile mass, which is a question of direct nuclear safeguards interest in the context of spoofing scenarios.

2. Model development

Consider an isolated bare piece of homogeneous plutonium compound, for example, a chunk of Pu metal or a cylindrical container holding PuO_2 powder. The spontaneous fission of the even Pu-isotopes provides an internal spatially uniform and isotropic source of initiating neutrons (we shall introduce (α, n) reactions later). Our objective is to obtain in an approximate way to estimate the importance of multiple scattering in the determination of the prompt neutron leakage self-multiplication factor for highly sub-critical masses of materials of interest to nuclear waste, nuclear safeguards, and neutron metrology applications (Ensslin et al., 1998; Croft and Henzlova, 2013; Croft and Favalli, 2017). We do so using a simple one-energy group, hybrid point-source model. Begin by introducing P_0 , the probability that a neutron will emerge from the item without undergoing a collision of any kind. Assume that if the neutron does interact there are just three interaction possibilities, which are: the neutron can be parasitically captured and removed with a microscopic cross-section σ_c , it can be elastically scattered (and in the one energy-group model no change of energy takes place) with a microscopic cross-section σ_s , or, it can induce fission with a microscopic cross-section σ_f . The overall or total microscopic cross-section is given by $\sigma_{tot} = (\sigma_c + \sigma_s + \sigma_f)$. For a given medium (mixture of nuclides) these cross-sections will be an appropriate linear combination of contributions as will become clear later in the worked example where the isotopic dependence will be made explicit. Capture excludes fission but includes (n, γ) , (n, α) , and all other reactions without a neutron in the final state. Conceptually $(n, 2n)$ and similar interactions with multiple neutrons in the final state can be treated as a special case of fission for our purposes and handled by adjusting both the fission cross section and the multiplicity distribution of neutrons emitted following induced fission. In practice, the chance of (n, xn) reactions is usually small and so we’ll not consider them further.

The probability that the first interaction of an individual neutron’s history will be a scatter event is given by Equation (1):

$$\vartheta = (1 - P_0) \bullet \frac{\sigma_s}{\sigma_{tot}} \quad (1)$$

Ignoring spatial dependence, the scattered neutron, according to the assumptions of the present model, behaves just like the initial neutron with the same chance of each type of interaction and so the probability after each scatter that the next (i.e. subsequent) event will be a scatter is assumed to be constant with the same value ϑ . Because of scattering, the influence of every initial source neutron is, therefore, in a sense, amplified so that the effective initiating-neutron population per starting particle, S , may be written as an infinite sum as follows:

$$S = 1 + \vartheta + \vartheta^2 + \vartheta^3 + \vartheta^4 + \dots = \frac{1}{1 - \vartheta} \quad (2)$$

Equation (2) quantifies our intuitive notion that neutrons that scatter travel further (that is have a longer cumulative flight-path length), on the average, inside an item and so have a greater probability of undergoing a nuclear reaction than neutrons that do not scatter. Numerically, each of these effective initiating neutrons has a chance of inducing fission with a probability given by $(1 - P_0) \bullet \frac{\sigma_f}{\sigma_{tot}}$ which is just the

analogue of our earlier scattering result. Thus, the probability, p_f , that a primary source neutron born inside the measurement item will induce a fission is given by:

$$p_f = \frac{(1 - P_0) \bullet \frac{\sigma_f}{\sigma_{tot}}}{(1 - \vartheta)} = \frac{(1 - P_0) \bullet \frac{\sigma_f}{\sigma_{tot}}}{1 - (1 - P_0) \bullet \frac{\sigma_s}{\sigma_{tot}}} = \frac{(1 - P_0) \bullet \sigma_f}{\sigma_{tot} - (1 - P_0) \bullet \sigma_s} \quad (3)$$

This expression can be adapted immediately to give the corresponding probability for parasitic capture:

$$p_c = \frac{(1 - P_0) \bullet \sigma_c}{\sigma_{tot} - (1 - P_0) \bullet \sigma_s} \quad (4)$$

Within this simple physical picture, the neutron at birth, and also following every scatter, has a probability P_0 of escaping from the body without interaction. The average overall probability, p_L , that the initial neutron will emerge, or leak, from the object allowing for multiple scattering is therefore given by the expression:

$$p_L = \frac{1}{(1 - \vartheta)} \bullet P_0 \quad (5)$$

In the limiting case of a pure scattering medium, $\sigma_s = \sigma_{tot}$, $\vartheta = (1 - P_0)$, $p_f = 0$, and $p_c = 0$ which leads to the result $p_L = \frac{P_0}{(1 - P_0)}$. In the special case $\sigma_s = 0$, $p_L = 1 - p_f - p_c = P_0$. This follows from the fact that true probabilities sum to unity and there are only three possibilities for how the neutron is removed from the population; it can leak (escape) from the sample, undergo fission, or undergo parasitic (non-fission) capture.

The expressions for p_f , p_c , and $p_L = (1 - p_f - p_c)$ describe how to estimate the overall interaction probabilities, and inclusive of (multiple) scattering for a small ('optically thin') but finite body. These estimates are used in the commonly used monoenergetic point-model equations, under the assumption that the true spatial distribution of scattered events does not significantly impact the results. The key to all this is having a way to estimate P_0 .

In the present discussion, the measurement items of interest all have finite fission cross-sections, are deeply subcritical and are in dynamic equilibrium ('steady state'). This is an important domain of nuclear materials safeguards. The fission process may therefore be described by the removal of the initial neutron and the liberation of an additional $\bar{\nu}$ neutrons on the average. We usually denote the mean number of prompt neutrons emitted following fission by $\bar{\nu}$ and refer to it as nu-bar in recognition of this traditional notation. By tallying the neutron-number balance overall neutron generations within the point-source model, a simple expression for the prompt neutron leakage self-multiplication can be derived. The result is stated below, and the details of the derivation can be found in (Ensslin et al., 1998; Croft et al., 2012a), and in the Appendix for further discussion:

$$M_L = \frac{1 - p_f - p_c}{1 - p_f \bar{\nu}} = \frac{1 - p_f \bullet \left(1 + \frac{\alpha_c}{\sigma_f}\right)}{1 - p_f \bar{\nu}} \quad (6)$$

The qualification 'prompt neutron' applies because delayed fission neutrons are not being considered. This is because they are emitted long after the prompt fission chain initiated by a spontaneous fission event has completed. In this respect the influence of delayed neutrons is similar to random (α, n) source neutrons (Croft and Favalli, 2017) in that on the time scales of the fission chains they may be treated as appearing randomly in time relative to the primary fission events.

In the limit when $(1 - p_f \bar{\nu})$ approaches zero from above (i.e., when $p_f \bar{\nu}$ approaches unity from below), the system approaches prompt criticality where neutron losses and gains just balance and the average neutron population would be expected to be self-sustaining once started (again, neglecting the contribution from delayed neutrons). Later, as a matter of convenience, we shall use bare-sphere critical masses for testing the model, although experimental nuclear safeguards work is usually concerned with the non-destructive assay of multiplying items,

such as nuclear fuel product storage cans, scrap, and containerized waste, with $p_f \bar{\nu} \ll 1$, which is to say, in mathematical terms, deeply sub-critical conditions.

From the preceding analysis, all the elements are now in place to evaluate the prompt neutron leakage self-multiplication factor M_L . We note that the expression for M_L depends on the scattering cross-section but that the dependence is implicit in that it enters via the detailed calculation of p_f . We observe that formally one may treat capture as a special case of fission without neutron emission and scattering as a fission event with the emission of one neutron, in which case one would need to mix cross-sections and compute $\bar{\nu}$ accordingly (see also the Appendix). However, there is no mathematical advantage in doing so for the present purposes which is why we have developed the model using explicit interaction cross sections which retains physical meaning. Within the one-energy group approximation inelastic scattering and any reactions with a single neutron in the final state are treated the same as elastic scattering because they do not change the number of neutrons in the system and in a one-energy group approximation, the energy difference between neutrons is not relevant. $(n,2n)$, $(n,3n)$ and similar processes are weak compared to (n,f) and will also be ignored here, but could be treated as special cases of fission with exactly two and three neutrons being emitted respectively. Expressed differently, the 'trick' to using a one-group treatment to good effect is to select appropriate average interaction cross sections.

Inserting the earlier expression for p_f into the above expression for M_L , after some re-arrangement, the following expression is obtained for M_L in terms of the un-collided escape probability, P_0 :

$$M_L = \frac{1}{1 - \left(\frac{1 - P_0}{P_0}\right) \bullet \left(\frac{\sigma_f(\bar{\nu} - 1) - \sigma_c}{\sigma_{tot}}\right)} \quad (7)$$

To proceed further an explicit way to estimate P_0 is needed. To begin we shall initially evaluate P_0 using the analytical result for a uniform isotropic spherical source. In doing so we shall see by extension that M_L results for other bodies can clearly be calculated provided P_0 can be estimated. Later we shall present a general scheme to calculate P_0 for cylinders which is more pertinent because storage containers for special nuclear materials are often cylindrical.

P_0 depends on the shape and size of the uniform body and also on the material properties through the neutrons mean free path (mfp) $\lambda = 1/\Sigma_{tot}$ the reciprocal of the total macroscopic neutron cross section. For a sphere of radius a the probability that a neutron will emerge without undergoing a collision is given by (Croft, 1990; Bell and Glasstone, 1970):

$$P_0 = \frac{3}{8x^3} [(1 + 2x)e^{-2x} + 2x^2 - 1] \quad (8)$$

where $x = \Sigma_{tot} a$ and Σ_{tot} is the total macroscopic cross-section averaged over the fission spectrum in our case because ^{240}Pu spontaneous fission and ^{239}Pu induced fission are usually assume to be the dominant neutron producers, and the average cross section is the appropriate interaction parameter for use in the one-energy group point model. Of course (α, n) neutrons are always present and a more sophisticated energy treatment is possible although we won't discuss that further. However, for pure PuO_2 oxides the $O(\alpha, n)$ neutrons have a broad spectrum with a mean energy close to that of fission neutrons and it is traditional to treat them as being in the same energy group. For context for pure PuO_2 the (α, n) -to-(SF, n) ratio is in the approximate range 0.4–1 depending on the isotopic composition of the Pu. The macroscopic cross-section is the product of the microscopic cross-section and the number density of targets (Huges, 1953; Fleming, 1982) and see also Lindstrom (Lindstrom and Fleming, 2008) for some corrections and subtle details in the use of mfp in relation to thermal neutron self-shielding. $x = a/\lambda$ is a natural dimensionless measure of the size of the sphere in multiples of the mfp. In the limit $x \ll 1$ the expression for P_0 can be expanded to obtain $P_0 \approx$

$1 - \frac{3}{4}x + \frac{2}{5}x^2$. We shall use this limiting case shortly.

Even within the limitations of the one energy-group model, whether the expression for M_L is useful or not depends on whether the escape probability following one or more scatterings remains numerically similar to P_0 or if the altered (compared to the spontaneous fission source) spatial distribution of neutrons exerts a strong influence on its value. For small bodies where scattering is not expected to matter much, one might imagine the approximation will work best because the likelihood for one or more scatterings is small. On this basis, to first order, we find for small spheres that:

$$(M_L - 1) \approx \frac{(\sigma_f(\bar{v} - 1) - \sigma_c)}{\sigma_{tot}} \frac{3}{4} x = (\Sigma_f(\bar{v} - 1) - \Sigma_c) \left(\frac{3}{4} a \right) \quad (9)$$

where Σ_f is the macroscopic fission cross-section, Σ_c is the macroscopic capture cross-section, and $\frac{3}{4}a$ is the mean geometrical flight path out of the sphere (Croft, 1990). If we call the mean geometrical flight path out of a body \bar{l} , then for small (in terms of the mfp) bodies the general expression:

$$(M_L - 1) \approx (\Sigma_f(\bar{v} - 1) - \Sigma_c) \bullet \bar{l} \quad (10)$$

holds as a reasonable approximation.

At this order of approximation, we see from the form of this expression that, as one might have anticipated at the onset, scattering does not influence the result, and so, for such deeply sub-critical problems, it seems that we have gone to a lot of trouble for no evident gain. But the definition of ‘small’ in the expansion of P_0 is that $x = \Sigma_{tot} \bullet a \ll 1$, and of course Σ_{tot} itself depends on the scattering cross-section. Thus, as the scattering cross-section is increased, the validity of the first-order result is notionally driven to smaller and smaller (and hence lower and lower mass) objects which could consequently limit its usefulness. As we shall show, for nuclear waste assay and for nuclear materials safeguards applications the items of concern are often of intermediate ‘thickness’ and so the full expression for M_L , rather than the limiting case, is more appropriate and this accommodates the small but finite influence of (multiple) scattering according to the approximate treatment described earlier.

We note that, according to the model so far developed, the influence of scattering is embodied in the behavior of the factor $\frac{1-P_0}{P_0}$ and that for uniform spherical objects P_0 is an analytic function of $\Sigma_{tot} \bullet a$. Thus, one can immediately appreciate that, in this simple picture of the self-multiplication process, the presence of scattering mimics the effect of increasing the material density, or increasing the radius of the sphere, or the product of the two by the factor $\left(1 + \frac{\sigma_s}{\sigma_c + \sigma_f}\right)$ over the case where the scattering cross-section is zero. For the reasons already explained, the simple model developed here cannot represent the true richness of the multiplying process taking place (i.e. a neutron’s fate depends on where it was born). But because the ratio $\frac{\sigma_s}{\sigma_c + \sigma_f}$ can exceed unity for the materials of interest it is apparent, based on the forgoing analysis, that scattering is likely to exert an important influence in certain situations of practical concern. The best way to illustrate this quantitatively is to work through some examples which will be done after developing an approach for more realistic cylindrically shaped objects.

It is also worth mentioning that a more involved description of the scattering effect is possible using a one-speed transport theory approach. Such a study was performed recently by Pázsit et al. (2023). The results confirm and demonstrate quantitatively that for high $\frac{\sigma_s}{\sigma_c + \sigma_f}$ ratios, scattering has a thorough effect, increasing largely the prompt neutron leakage self-multiplication, as well as the higher order factorial moments of the number of emitted neutrons. The space-dependent model is capable of accounting for the ‘reflector effect’ of scattering, which in turn leads to increase internal multiplication. Its disadvantage is that the mentioned factorial moments underpinning the various correlated

counting rates, including the prompt neutron leakage self-multiplication, are solutions of integral transport equations, which cannot be obtained analytically, only numerically (Pázsit et al., 2023).

3. Extension to cylindrical bodies

The approach developed for spheres can be readily extended to simple bodies of other shapes. Real measurement items are often in the form of cylindrical cans. Cylindrical bodies are therefore a natural shape to consider. Whereas the escape path distribution is a single parameter distribution the cylinder requires two parameters (scale and aspect ratio) to define it. Bell and Glasstone (1970) present an excellent discussion of escape probabilities in the framework of Dirac’s chord method, introduced in 1943 (Dirac, 1943; Dirac et al., 1943). A key result is the behavior in the limit that the dimensions of a non-re-entrant body containing a uniform and isotropic neutron source are large compared to the neutron mfp $\lambda = 1/\Sigma_{tot}$, (see section 2), the result for P_0 is $P_0 = \frac{1}{4} \frac{S \bullet \lambda}{V}$, where S is the surface area and V is the volume of the body. Numerically, in this limit, P_0 is equal to the fraction of neutrons generated within a quarter of the mfp from the surface. The geometry of the body is completely defined by the probability distribution function $p(R)$ of chord lengths and the un-collided escape probability P_0 is given by the integral:

$$P_0 = \frac{1}{\bar{R} \Sigma_{tot}} \int_{R=0}^{\bar{R}_{max}} p(R) \cdot (1 - e^{-\Sigma_{tot} R}) \cdot dR \quad (11)$$

where $\bar{R} = 4 \frac{V}{S}$ is the mean chord length and the bar notation when appearing above a parameter denotes the mean formed over the chord length distribution (CLD) $p(R)$.

For certain simple bodies, such as the sphere (already discussed), slab and infinite cylinder (Fleming, 1982; Lindstrom and Fleming, 2008; Case et al., 1953) closed form expressions for $p(R)$ can be found allowing P_0 to be evaluated analytically. For other bodies fully numerical evaluation of the un-collided escape probability P_0 may be readily calculated by integrating the probability of no collision of a neutron from a point r in space with given velocity directions μ and φ , where μ is the cosine of the polar angle, and φ the azimuthal angle, until the surface of the item. For a circular right cylinder with radius R and height H , P_0 is given as:

$$P_0 = \frac{1}{2\pi R^2 H} \int_0^R r dr \int_0^H dh \int_{-1}^{+1} d\mu \int_0^{2\pi} e^{-\Sigma_{tot} \ell(r,h,\mu,\varphi)} d\varphi \quad (12)$$

Here, $\ell(r, h, \mu, \varphi)$ is the distance from the point (r, h) along the direction (μ, φ) to the surface of the cylinder, which can be given in analytical form for all simple geometries. Numerical values of P_0 for cylinders of various sizes and aspect ratios are given in (Pázsit and Dykin, 2022).

Continuing with the analytical approximation, expanding the integral (Equation (11)) for P_0 and evaluating it term by term an equivalent series representation is obtained:

$$P_0 = 1 - \frac{1}{2} \frac{\bar{R}^2}{\bar{R}} (\bar{R} \cdot \Sigma_{tot}) - \frac{1}{6} \frac{\bar{R}^3}{\bar{R}^3} (\bar{R} \cdot \Sigma_{tot})^2 + \dots \quad (13)$$

For a given body shape, the factors $q_{n-1} = \frac{1}{n!} \frac{\bar{R}^n}{\bar{R}^n}$, where q_{n-1} is the coefficient of the $(\bar{R} \cdot \Sigma_{tot})^{n-1}$ term in the polynomial expansion for P_0 in terms of $\bar{R} \cdot \Sigma_{tot}$, are just numerical constants, and the product $\bar{R} \cdot \Sigma_{tot}$ represents a dimensionless measure of the average or characteristic size of the body in multiples of the mfp. For solid convex 3-D bodies $\bar{R}^3 = (12/\pi)V^2/S$, but this, along with $\bar{R} = 4 \frac{V}{S}$, are the only two moments of the CLD that can be expressed in terms of simple geometric properties (Larsen, 1980; Mazzolo et al., 2003; Mazzolo and Roesslinger, 2003). The others must be found numerically unless, as in the case of the sphere, the CLD is both known and algebraically amenable (Croft, 1990; Gorshkov and Tsvetkov, 1962). What this form for the evaluation of P_0

tells us that a polynomial representation in powers of $\bar{R} \cdot \Sigma_{tot}$ is a natural choice. In the limit of small bodies, as $\bar{R} \cdot \Sigma_{tot}$ approaches zero, we observe that P_0 approaches unity linearly. As defined here q_0 is half the ratio of the mean square chord length to the square of the mean chord length, and q_0 is therefore least for a sphere with a value of $9/16 \approx 0.5625$. In discussing the effect of holes on the streaming of neutrons in a nuclear reactor (Behrens, 1949) has noted that for all ‘reasonable shapes’ q_0 varies only between fairly narrow limits seldom exceeding about $5/6 \approx 0.8333$ (although shapes offering very long chords over a finite solid angle can in principle raise q_0 without limit – for instance in the case of a collimated beam directed along an infinitely long cylindrical channel). On this basis an approximate rule of thumb for the rough estimation of P_0 for neutronically ‘thin’ bodies is to use the formula for a sphere with the same mean chord value. For squat bodies (meaning that the dimensions in all directions are about the same), such as the cube or a cylinder with diameter equal to the length, this approximation should work reasonably well. However, it is clear that the q -coefficients of the expansion are shape dependent and that in using the spherical model for other shapes will inevitably lead to some error (bias or model mismatch), even for small bodies, as witnessed and quantified by the spread in q_0 values given for ‘reasonable’ shapes (Behrens, 1949).

Because analytical expressions for P_0 can only be derived in closed form in terms of standard functions for a few shapes (Case et al., 1953) it is convenient to have a simple albeit approximate expression which can be used over a wider range and especially for important shapes such as the cylinder. A simple function with the correct extreme-small and extreme-large body behavior is known as the Wigner Rational Approximation (WRA) (Wigner et al., 1955; Creutz et al., 1955) and provides a rough means to calculate P_0 for arbitrarily shaped and sized non-re-entrant homogeneous bodies containing a uniform isotropic emitter. The form of the WRA is as given in Equation (14):

$$P_0 \approx \frac{1}{1 + 4 \frac{1}{\Sigma_{tot}}} = \frac{1}{1 + \bar{R} \cdot \Sigma_{tot}} \quad (14)$$

The WRA works quite well for first order calculations (Pashkin, 1970) and with specific piece-wise ad-hoc shape and size dependent modifications, that add to the level of algebraic complexity, agreement to a fraction of one per cent over the full dynamic range can be achieved for the plane, infinite cylinder and sphere geometries (e.g. the work of Otter referenced in Landers (Landers et al., 1998)). The WRA works as well as it does despite its simplicity because the escape probability integral is not very sensitive to the CLD function. However, we shall not use the WRA explicitly in our calculations, but we mention it so as to invoke it as part of a plausibility argument for an interpolation scheme to be described next for the estimation of the un-collided escape probability of finite cylinders. This is an important case because, as already noted, in nuclear safeguards very often the assay item is cylindrical, for example PuO_2 or mixed UO_2 - PuO_2 product powders are commonly kept in cylindrical storage canisters. Sauer (1963) has pointed out that for long (compared to the diameter) circular right cylinders (such as nuclear fuel rods) with intermediate values of $\bar{R} \cdot \Sigma_{tot}$ the WRA is up to 18% low. Sauber approached the problem of getting a better, yet still analytically simple, representation in a rather general way by introducing a class of one-parameter peaked CLDs defined only by \bar{R} and a body dependent geometrical index α . The resulting expression for the un-collided escape probability under Sauber’s scheme becomes:

$$P_0 \approx \frac{1}{\bar{R} \cdot \Sigma_{tot}} \left\{ 1 - \frac{1}{[1 + \bar{R} \cdot \Sigma_{tot}/(\alpha + 1)]^{(\alpha+1)}} \right\} \quad (15)$$

Setting $\alpha = 0$ we recover the original WRA. With $\alpha = 3.58$ Sauber found that his formula agreed with the exact results for an infinite cylinder with an error no larger than 0.6% over the full range $\bar{R} \cdot \Sigma_{tot} \in [0, \infty]$. This is a significant improvement over the WRA and yet remains analytically simple and general for practical implementation. For finite

circular cylinders Gubbins (Gubbins et al., 1964) lues along with the associated statistical sampling uncertainty using the Monte Carlo method including for a squat circular cylinder (with diameter d equal to the height h) over the range $d \cdot \Sigma_{tot} = 0.1$ to 17 (i.e. $\bar{R} \cdot \Sigma_{tot} = 0.067$ to 11.3). Performing a chi-squared minimization we find that Sauber’s formula represents the numerically calculated ‘exact’ P_0 values to better than 1% over the entire range with the geometrical index α set to 2.41.

The question now becomes how to interpolate between these two cases, namely the case of the infinitely long circular cylinder discussed by Sauber and the squat circular cylinder (with $d = h$) discussed by Gubbins. Introducing the aspect ratio $z = h/d$ the mean chord of a finite cylinder can be written as follows:

$$\bar{R} = d \cdot \frac{2z}{1 + 2z} = d \cdot \frac{1}{1 + \frac{1}{2z}} \quad (16)$$

In the limit that z tends to infinity note that \bar{R} tends to d .

Note too that the WRA expression can be re-written in the following way:

$$\frac{1}{P_{coll}} = \frac{1}{1 - P_0} = \frac{d \cdot \Sigma_{tot} + 1 + \frac{1}{2z}}{d \cdot \Sigma_{tot}} \quad (17)$$

where $P_{coll} = (1 - P_0)$ is the probability that the neutron will not escape un-collided but will suffer at least one interaction. Expressed this way the WRA suggests that the difference between the reciprocal values of $(1 - P_0)$ scales linearly with one-half the reciprocal of the aspect ratio z . We have already established approximate relationships for two special cases, $P_{0,\infty}$, the infinite circular cylinder with $z = \infty$ and the squat cylinder $P_{0,1}$ with $z = 1$ using Sauber’s formula. Thus, an interpolation scheme of the form proposed by Gubbins for a finite cylinder, with obvious notation, takes the form:

$$\frac{1}{(1 - P_{0,z})} = \frac{1}{(1 - P_{0,\infty})} + \frac{1}{z} \left[\frac{1}{(1 - P_{0,1})} - \frac{1}{(1 - P_{0,\infty})} \right] \quad (18)$$

where for the present purposes it is understood that $z = (h/d)$, and the value of $P_{0,\infty}$ is to be evaluated using Sauber’s formula with $\alpha = 3.58$ and the value of $P_{0,1}$ is to be evaluated with Sauber’s formula with $\alpha = 2.41$.

Accordingly, the un-collided escape probability for all finite cylinders of practical interest can be estimated. To test the accuracy of this interpolation scheme we compared the results against the computed results of Gubbins for $d \cdot \Sigma_{tot}$ equal to 0.01, 1 and 11, and for each case with z equal to 2, 4 and 8. Additional data sets were also taken from Carlvik, 1967a¹, 1967b. The data set of Foell, Berner and Tong which are reproduced by Carlvik covers the range $d \cdot \Sigma_{tot}$ equal to 0.8, 2, 4, 6, 8, and 12 with z equal to 2. McLeod’s data set, which is also reported in Carlvik (Carlvik, 1967a, 1967b; McLeod, 1963), covers the $d \cdot \Sigma_{tot}$ range from 0.001 to 20 with z equal to 1 and 10. In all cases good agreement is obtained.

Computationally efficient and accurate numerical sampling methods for the computation of collision probabilities for other homogeneous 3-dimensional bodies have recently been developed (Garcia, 2004). Another straightforward and effective approach based on the numerical integration of the non-collision probability, mentioned earlier, and described for cylinders in Eq. (12), is also applicable for arbitrary geometries (Pázsit and Dykin, 2022). Hence by using similar methods to those described here, or some other application specific motivated interpolation approach, results for shapes other than the sphere and

¹ . Note the final line of Equation (4) in this article should be replaced by:

$$\frac{h^2 \cdot d}{2} \left\{ \ln \left(\frac{d}{h} + \sqrt{1 + \left(\frac{d}{h} \right)^2} \right) + \frac{d}{h} \sqrt{1 + \left(\frac{d}{h} \right)^2} - \left(\frac{d}{h} \right)^2 \right\}$$

cylinder can also be developed as needed. For more complex bodies, for example a randomly dispersed distribution of pieces of nuclear material embedded in a matrix, more complex Monte Carlo chord length sampling strategies have been used devised (Liang and Ji, 2011), but this takes us far outside our intended scope and will not be discussed further here. The important point is that the purely geometrical parameters can be computed in various ways and to arbitrary accuracy and so in principle and in practice do not limit the implementation of the multiplication model.

4. Worked examples

In developing the expression for the prompt (one fast, internal, neutron energy-group) leakage self-multiplication factor M_L , we assumed an isolated point-like source of monoenergetic neutrons with a spatially flat and isotropic emission profile. These choices are most likely to lead to an approximation most suitable for weakly multiplying, that is to say ‘neutronically thin’, bodies with a size small compared to the neutrons mean free path. However, we are compelled to calculate interaction probabilities for finite bodies of a certain shape for practical applications – in our case expressions for a sphere and a circular cylinder have been explicitly presented. As noted, cylindrical containers and shapes are commonly used to store product materials safeguards in highly sub-critical states but the spherical case may be used below as an extreme benchmark because critical mass values are readily available in the literature.

To define the application space the remaining major challenge is how to select suitable cross-sections and the other necessary nuclear data values to be inserted into the expressions already developed (Croft et al., 2011). It seems reasonable to use quantities averaged over a representative fission neutron spectrum because the prompt fission neutron spectrum from ^{240}Pu and that of induced fission are similar, although we recognize that generating representative nuclear data is an area which justifies far more detailed analysis than can be covered here. The detailed computational results of Pearlstein (1996) for the ^{239}Pu -metal system at criticality provide some support for this assumption. In particular, for those conditions, the neutron spectrum in a solid ^{239}Pu metallic sphere of critical mass was found to be nearly a pure fission spectrum (described in Pearlstein’s study by a Maxwellian shape with a temperature parameter of 1.39 MeV) with only about 0.5% of the neutrons below 0.1 MeV. The leakage fraction was given as 0.674 and the median fission energy as 1.63 MeV. The neutron reproduction factor, η , the average number of fission neutrons ejected per absorption ($\eta = \frac{\bar{\nu}}{1 + \sigma_c/\sigma_f}$) was estimated as 3.08. Furthermore, the gross similarity in the cross-sections of the fissile actinides and of the fissionable actinides, respectively, noted by Pearlstein is also helpful in that it hints at the possibility that the results will not be extremely sensitive to isotopic composition for some broad categories of materials, especially given we are concerned only with unmoderated (that is dry) nuclear fuel product items. It is noteworthy in this context that (α, n) reactions on oxide materials results in a broad spectrum with a mean energy of about 2 MeV which is comparable to the mean fission energy.

Cross-section data averaged over a nominal ^{235}U thermal-neutron induced fission differential energy spectrum described by the Watt shape $\exp(-E/a) \cdot \sinh(\sqrt{bE})$, with $a = 0.988$ MeV and $b = 2.249$ MeV $^{-1}$ over the interval 10^{-5} to 20 MeV are conveniently available for ENDFB/V data (Magurno et al., 1982). We are not aware of a similarly convenient source of fission spectrum and cross-section (i.e. fission spectrum reaction) weighted nu-bar values for the various nuclides of interest to safeguards, nor of similar data for more recent ENDFB files. For simplicity, and for the purposes of illustration only, we have scaled values off the energy dependent plots presented in the review of Maslov et al. (Maslov et al., 2008) at 2 MeV – roughly the mean fission neutron energy. This is a reasonable choice in the sense that nu-bar following fission typically varies approximately linearly with incoming neutron

energy, although on the other hand in doing so we are neglecting the variation with energy of the fission cross-section when folded with the spectrum. Since in the MeV region uncertainties are typically in the region of 3–5 %, and given the other approximations we are making, we shall not concern ourselves with the additional 1% or so of delayed neutrons that are emitted at relatively long times after the fission event but are crucially important for reactor control (Walker and Weaver, 1979). Also, implicit in the present discussion is that the neutrons emitted are uncorrelated in either energy or direction with one another, which although perhaps not strictly true is very nearly so, and so is a valid assumption in the context of the present discussion (Wilson, 1947; Gavron, 1976) given the other approximations. Additionally, first, second and third chance fission (n, nf), ($n, 2nf$), and ($n, 3nf$) and ($n, 2n$) reactions are assumed to be rolled up into one ‘effective’ fission process.

It is also necessary to make an allowance for the manifestation of anisotropic neutron scattering and the energy loss associated with inelastic scattering. The monoenergetic model described cannot accommodate this directly but the effects can be inserted by picking appropriate effective interaction cross-sections. We observe that scattered fission neutrons travel preferentially in the forward direction. In the extreme case of a scattered neutron that goes straight-on after interacting, it is as if the scatter never took place, and so, for the purposes of estimating the multiple scattering effect discussed above, the influence of elastic scattering as a physical process of consequence is reduced. Borrowing from neutron transport theory and examining under what conditions elementary diffusion theory emerges from it (Bell and Glasstone, 1970; Glasstone and Edlund, 1957), one way to approximately account for anisotropic scattering (before going to the complexity of P_n treatments with $n > 0$) is to define a reduced or effective isotropic scattering transport cross-section with a value given by $\sigma_s \cdot (1 - \bar{\mu})$, where $\bar{\mu}$ is the average value of the cosine of the neutron scattering angle between the initial and final direction in the laboratory reference frame. We do not know of a convenient source of pre-processed fission spectrum reaction weighted $\bar{\mu}$ values for the actinides and so for now, purely for illustrative purposes, we adopt a value of $\bar{\mu} \sim 0.6$ which is consistent with the value obtained from an empirical analysis of natural uranium fuel rod experiments. A very rich survey of inelastic scattering remains in the early studies (Langsdorf et al., 1956, 1957; Lovchikova, 1962), which can be used to inform the choice of $\bar{\mu}$ over much of the periodic table. For the other scattering targets of interest here (oxygen, fluorine and gallium, for example, which may be present in common compounds and alloys found in the fuel cycle) we make the approximation that the scattering is isotropic in the center-of-mass frame and use the approximate formula $\bar{\mu} = \frac{2}{3A}$, (Bell and Glasstone, 1970; Glasstone and Edlund, 1957), where A is the ratio of the mass of the target to the mass of the neutron and is sufficiently close in value to the molar mass for our calculational purposes.

The use of a one-energy group approximation also poses another challenge because in reality we can expect the subsequent influence (or importance) of inelastically scattered neutrons to be changed because neutrons shifted to lower energies will no longer have the same interaction probability (cross-section) for inducing fission. The cross-section could go higher or lower, depending on the nuclear species present. Equally significant is the dependence of the $\bar{\nu}$ of induced fission on the energy of the neutron. As previously mentioned, $\bar{\nu}$ decreases monotonically as the incident neutron energy decreases. Consequently, neutrons that have undergone inelastic scattering will yield fewer neutrons upon fission. Actinides containing an even number of neutrons (the fissionable or fertile nuclides) characteristically have an effective fission energy-threshold (Bierman and Clayton, 1969). The classic example in natural and low enriched uranium reactor fuel is the drop in fast neutron fission in ^{238}U which has an effective fission threshold of about 1 MeV or so, with a very small fission cross-section below this. For comparison, in the case of ^{237}Np the fission threshold is about 0.5 MeV (Sanchez, 1997). Evaluating this effect, especially across a mixture of nuclides comprising

an assay item, is beyond the scope and intent of the present discussion which is concerned mainly with the development of the general framework not the optimization of its application, but it is a common problem in reactor physics and the lattice code tools developed for that arena could be employed. For convenience here we shall simply assume that the true inelastic cross-section can be replaced by the product $s \cdot \sigma_{in}$ where s is a suitable scale factor. Lacking additional guidance (which could also come from either experimental data or from detailed Monte Carlo simulation to provide the necessary averaging of microscopic evaluated nuclear data in representative case) to proceed with our pedagogic journey based on the literature cited we make a guess at the value of s setting it to a value of about 0.8 for all fertile nuclides and a value of unity for all of the fissile nuclides. This choice could alternatively be adjusted in a crude integral sense to reproduce the known bare critical mass values which are large objects and more sensitive to such effects. We re-iterate that a future study aimed at obtaining spectrum average nuclear data for use with the present simplified transport model is needed.

Table 1 Gives a short list of calculated prompt critical masses for unreflected metal spheres based on the calculations of Wright et al. (2000). These authors provide critical masses covering all the nuclides considered in this paper (and many more) based on ENDF/B-V and -VI libraries – which when using ENDF/B-V average cross section provides a kind of self-consistency.

To illustrate the use of the model some results are presented in **Table 2** for a selection of cases based on the default parameters explained in the text, which recall are: fission spectrum average cross sections; 2 MeV nu-bar values; $s = 1$ or 0.8; and $\bar{\mu} = \frac{2}{3A}$ or 0.6. The example cases are as follows:

Case I: Weapons grade Pu-alloy spheres. The alloy comprised 1 wt% Ga, with a Pu-isotopic composition $^{238-242}\text{Pu}$ of 0.012, 93.788, 5.926, 0.241, and 0.033 wt%, respectively, and with 0.1 wt% ^{241}Am with respect to ^{241}Pu . The density was taken as 15.3 g cm^{-3} .

Case II: As Case I but in cylindrical form with $\text{Diameter}=\text{Height}$.

Case III: As Case II but with the Pu-isotopics replaced by a reactor grade with composition $^{238-242}\text{Pu}$ of 2.5, 51.3, 24.2, 15.1, and 6.9 wt%, respectively, and no ^{241}Am .

Case IV: As Case III but with the $\text{Diameter}=2 \times \text{Height}$.

Case V: As Case IV but with the Pu without Ga and in the form of PuO_2 with a powder density of 3.0 g cm^{-3} .

Case VI: As Case V but with the density of 2.5 g cm^{-3} .

Case VII: As Case VI but with the PuO_2 replaced by mixed oxide (MOX) made up of a mixture of PuO_2 and UO_2 with a Pu to (Pu + U) mass ratio of 0.10. The isotopic composition of the depleted uranium $^{234, 235, 238}\text{U}$ was 0.00074, 0.20000, and 99.79926 wt%, respectively.

In all cases the leakage self-multiplication factors are tabulated as against total Pu mass in grams. These few examples were chosen to show how a sphere and a squat cylinder are similar, illustrate the impact of

Table 1

Critical masses in kg for unreflected bare metal spheres of selected nuclides for the densities indicated at room temperature. The critical mass data comes from Wright et al. (2000). The final column provides a rough indication of the variation one encounters in these values quoted across a selection of contemporary and recent published literature and is provided purely as a rough indication of the uncertainty in the calculated results.

| Nuclide | Density, g.cm ⁻³ | ENDF/B-V, kg | ENDF/B-VI, kg | Variation, kg |
|---------|-----------------------------|--------------|---------------|---------------|
| 233U | 19.05 | | 15.52 | 0.4 |
| 235U | 19.05 | | 46.50 | 0.2 |
| 237Np | 20.476 | 68.2 | 62.69 | 10 |
| 238Pu | 19.840 | 9.62 | 9.75 | 0.2 |
| 239Pu | 19.851 | 10.12 | 10.10 | 0.1 |
| 240Pu | 19.934 | | 36.95 | 3 |
| 241Pu | 19.840 | | 13.02 | 1 |
| 242Pu | 20.101 | | 85.35 | 5 |
| 241Am | 13.660 | | 60.04 | 2 |

Table 2

Leakage self-multiplication factors calculated using the model developed in the present work, and using the associated default parameters suggested, for the seven example Cases (I-VII) described in the text.

| Pu Mass, g | Case I | Case II | Case III | Case IV | Case V | Case VI | Case VII |
|------------|--------|---------|----------|---------|--------|---------|----------|
| 0.1 | 1.013 | 1.013 | 1.012 | 1.011 | 1.003 | 1.003 | 1.001 |
| 0.3 | 1.018 | 1.018 | 1.017 | 1.015 | 1.005 | 1.004 | 1.002 |
| 1 | 1.028 | 1.028 | 1.025 | 1.023 | 1.007 | 1.006 | 1.003 |
| 3 | 1.041 | 1.041 | 1.037 | 1.034 | 1.010 | 1.009 | 1.004 |
| 10 | 1.062 | 1.062 | 1.056 | 1.052 | 1.016 | 1.014 | 1.006 |
| 30 | 1.093 | 1.093 | 1.084 | 1.077 | 1.023 | 1.020 | 1.008 |
| 100 | 1.149 | 1.147 | 1.132 | 1.121 | 1.034 | 1.030 | 1.012 |
| 300 | 1.235 | 1.229 | 1.205 | 1.187 | 1.051 | 1.045 | 1.018 |
| 1000 | 1.414 | 1.396 | 1.350 | 1.315 | 1.079 | 1.069 | 1.028 |

changing plutonium grade, show the influence of aspect ratio, of density and of chemical form.

The choice of a spherical geometry is a natural one because the distribution of escape path-lengths is particularly simple - being both analytic and governed by just one geometry parameter. The sphere is special because the leakage self-multiplication factor for a given mass of homogeneous material is the largest of any shape because the volume to surface area is the least. The spherical geometry is also a common choice in elementary reactor theory textbook examples and furthermore spherical Pu items have been studied before in relation to the spatial variation of the leakage self-multiplication and its impact on quantitative neutron multiplicity counting (Göttsche and Kirchner, 2015).

According to the U.S. DOE weapons grade Pu as produced by low burnup of uranium fueled nuclear reactors typically contains about 93 wt% ^{239}Pu (U.S. DOE, 1997). Our choice of low burnup Pu isotopic composition is invented but falls into this category and is close to the compositions used to create calibration standards for nondestructive assay equipment as described by Crossley et al. (1994) and Hsue et al. (1997).

The number of possibilities is endless and so for convenience the mixing of cross sections and computations has been implemented in an easy-to-use Microsoft Excel spreadsheet (available from the authors). For completeness the default parameter set is shown in **Table 3**.

Using these nominal values, it is interesting to compare the estimated bare sphere critical mass values predicted against the accepted values listed previously in **Table 1**. This is done in **Table 4**. Although the model developed in the text is not expected to hold for such large items, and the model calculation is based on nominal and not selected or adjusted data parameters, the general level of agreement is reasonably good, especially for the Pu-isotopes and ^{241}Am . In a carefully curated learning environment this provides a topic of discussion and an opportunity to explore the impact of scattering $\bar{\mu}$ and s-factor choices, for example.

5. Conclusions

The point-model has been the cornerstone of neutron correlation counting development and application since Feynman, Rossi, de Hoffman and other luminaries analyzed the first critical experiments during the Manhattan Project at Los Alamos. It is perhaps surprising, therefore, that an extension of the point-model concept allowing for a simple quantitative forward calculation of leakage self-multiplication has not been developed as part of the associated scholarly tradition. To address this, in the present work, we have adapted how the fast fission effect in lumps of fuel was first calculated so as to complete the point-model view of neutron correlation counting. The predictive estimate of the leakage self-multiplication factor was constructed in the framework of the one energy group point model making use of an approximation for the uncollided escape probability to account for neutron scattering. The selection of nuclear data is based on simple and intuitive ideas supported by general surveys of nuclear properties although group average neutron

Table 3

Default data parameters used in the present implementation of the leakage self-multiplication model described. The number of significant figures shown for the values of the interaction cross sections exceeds the accuracy to which they are known in the context of the present model and associated assumptions.

| Nuclide | A_{mol} g.mol ⁻¹ | σ_s | $\bar{\mu}$ | σ_{inel} b | s-factor | σ_c b | $\sigma_{s,eff}$ b | σ_f b | σ_{tr} b | $\bar{\nu}$ n.fis ⁻¹ |
|-------------------|-------------------------------|------------|-------------|-------------------|----------|--------------|--------------------|--------------|-----------------|---------------------------------|
| O | 15.9994 | 2.782 | 0.041668 | 0.003138 | 1 | 0.009 | 2.669217 | 0 | 2.678217 | 0 |
| F | 18.9984 | 2.649 | 0.035091 | 0.938 | 1 | 0.017 | 3.494045 | 0 | 3.511045 | 0 |
| Ga | 69.723 | 2.723 | 0.009562 | 1.1103 | 1 | 0.019 | 3.807264 | 0 | 3.826264 | 0 |
| ²³³ U | 233.0396 | 4.781 | 0.6 | 0.8997 | 1 | 0.0595 | 2.8121 | 1.9058 | 4.7774 | 2.72 |
| ²³⁴ U | 234.0409 | 5.297 | 0.6 | 1.8106 | 0.8 | 0.1757 | 3.56728 | 1.2267 | 4.96968 | 2.63 |
| ²³⁵ U | 235.0439 | 4.803 | 0.6 | 1.4706 | 1 | 0.1053 | 3.3918 | 1.2351 | 4.7322 | 2.62 |
| ²³⁶ U | 236.0456 | 5.355 | 0.6 | 1.9561 | 0.8 | 0.1818 | 3.70688 | 0.5901 | 4.47878 | 2.6 |
| ²³⁸ U | 238.0508 | 4.818 | 0.6 | 2.577 | 0.8 | 0.0858 | 3.9888 | 0.3052 | 4.3798 | 2.64 |
| ²³⁸ Pu | 238.0496 | 4.633 | 0.6 | 0.8245 | 0.8 | 0.1507 | 2.5128 | 1.9768 | 4.6403 | 3.12 |
| ²³⁹ Pu | 239.0522 | 4.628 | 0.6 | 1.2463 | 1 | 0.0438 | 3.0975 | 1.7909 | 4.9322 | 3.15 |
| ²⁴⁰ Pu | 240.0538 | 4.617 | 0.6 | 1.552 | 0.8 | 0.089 | 3.0884 | 1.352 | 4.5294 | 3.14 |
| ²⁴¹ Pu | 241.0568 | 4.631 | 0.6 | 1.7911 | 1 | 0.1307 | 3.6435 | 1.5972 | 5.3714 | 3.2 |
| ²⁴² Pu | 242.0587 | 5.053 | 0.6 | 1.6947 | 0.8 | 0.0796 | 3.37296 | 1.1257 | 4.57826 | 3.1 |
| ²⁴¹ Am | 241.0568 | 4.747 | 0.6 | 1.5106 | 0.8 | 0.2619 | 3.10728 | 1.4655 | 4.83468 | 3.45 |
| ²³⁷ Np | 237.0482 | 4.584 | 0.6 | 1.6779 | 0.8 | 0.1678 | 3.17592 | 1.3473 | 4.69102 | 2.8 |

Table 4

Comparison of the accepted critical mass values taken from Table 1 against the values estimated using the simple model developed in the text albeit for much smaller items. The values in brackets indicate the plausible spread in the least significant figure.

| Nuclide | Accepted Value, kg | Model Value, kg |
|-------------------|--------------------|-----------------|
| ²³³ U | 15.5(4) | 22.7 |
| ²³⁵ U | 46.5(2) | 90.3 |
| ²³⁷ Np | 63(10) | 51.5 |
| ²³⁸ Pu | 9.8(2) | 12.5 |
| ²³⁹ Pu | 10.1(1) | 14.4 |
| ²⁴⁰ Pu | 37(3) | 33.0 |
| ²⁴¹ Pu | 13(1) | 19.3 |
| ²⁴² Pu | 85(5) | 55.8 |
| ²⁴¹ Am | 60(2) | 45.5 |

interaction data could be generated in other ways. In addition to providing a useful semi-intuitive mental framework for students and practitioners, our approach also introduces the elegance and ultimately the necessity of Monte Carlo simulation in a natural way but without requiring access to or training in such specialist computer codes to progress. The results are none-the-less of potentially practical value in cases where quick estimates or simple interpolations are needed for known geometries (e.g. in place of the known (α, n) assumption) assays of containerized plutonium compounds. For dry, fast-neutron systems of Pu and U (e.g. mixed oxide product) it explains why the leakage self-multiplication is quite insensitive to isotopic composition, and it describes the scaling with density and chemical form. Future work to refine the table of default parameters and to compare the performance of the

Appendix A. – Master Equation Considerations

Assuming the probabilities of the elementary processes are known and independent (i.e. Markovian) one has the equation for the probability distribution, $p(n)$, of the number of neutrons leaving the sample by one starting neutron as (Pázsit et al., 2009; Pázsit et al., 2023; Pázsit and Dykin, 2022; Pázsit and Pal, 2007):

$$p(n) = P_0 \delta_{n,1} + (1 - P_0) \frac{\sigma_c}{\sigma_{tot}} \delta_{n,0} + (1 - P_0) \frac{\sigma_s}{\sigma_{tot}} p(n) +$$

$$(1 - P_0) \frac{\sigma_f}{\sigma_{tot}} \sum_{k=0}^{\infty} f(k) \sum_{n_1+n_2+\dots+n_k=n} \prod_{l=0}^k p(n_l) \quad (A1)$$

where $f(k)$ is the number distribution of neutrons release following induced fission. From this master equation all other properties about the time evolution of the system can be derived. Introducing the generating functions:

simple model against detailed transport simulations. For example future workers might want to consider specifically low burnup (Pu + Am), or high burnup (Pu + Am), or reactor grade MOX. We would encourage and support such projects.

CRedit authorship contribution statement

Stephen Croft: Writing – original draft, Formal analysis, Conceptualization. **Andrea Favalli:** Writing – review & editing, Validation, Formal analysis, Data curation. **Malcolm Joyce:** Writing – review & editing. **Imre Pázsit:** Writing – review & editing, Methodology. **Melissa Styth:** Writing – review & editing, Validation.

Declaration of competing interest

The authors declare that they have no known competing financial interests or personal relationships that could have appeared to influence the work reported in this paper.

Acknowledgements

S.C. warmly acknowledges support from Lancaster University and A. F. gratefully acknowledges the support of the Joint Research Centre of the European Commission. M.S. acknowledges the grant from the EPSRC Centre for Doctoral Training in Nuclear Energy- GREEN (Growing skills for Reliable Economic Energy from Nuclear, grant number EP/S022295/1).

$$g(z) = \sum_{n=0}^{\infty} p(n)z^n \quad \text{and} \quad q_f(z) = \sum_{k=0}^{\infty} f(k)z^k \quad (\text{A2})$$

Eq. (A2) becomes:

$$g(z) = P_0 z + (1 - P_0) \left(\frac{\sigma_c}{\sigma_{tot}} + \frac{\sigma_s}{\sigma_{tot}} g(z) + \frac{\sigma_f}{\sigma_{tot}} q_f[g(z)] \right) \quad (\text{A3})$$

where in the last term on the right-hand side, $g(z)$, is the argument of the generating function $q_f(z)$.

Since, by definition, M_L is the expected number of neutrons leaving the sample, i.e.

$$M_L = \bar{n} = \left. \frac{\partial g(z)}{\partial z} \right|_{z=1} \quad (\text{A4})$$

an algebraic equation can be obtained for M_L by differentiating (A3) with respect to z which, when solved for \bar{n} yields the result:

$$M_L = \frac{P_0 \sigma_{tot}}{\sigma_{tot} - (1 - P_0)(\sigma_s + \bar{\nu} \sigma_f)} = \frac{P_0}{1 - (1 - P_0) \left(\frac{\sigma_s + \bar{\nu} \sigma_f}{\sigma_{tot}} \right)} \quad (\text{A5})$$

Eq. (A5) is identical to Eq. (6), although it is not immediately seen, rather it requires some algebra. The reason is that in (A5), only the probability of the first reaction occurs, whereas in (6), the leakage multiplication is expressed with the total probabilities that a neutron will induce fission (or will be captured).

It is also easily seen that Eq. (A5) can be brought into a form, which is the complete analogue of the ‘‘classic’’ formula (Ensslin et al., 1998; Croft et al., 2012a):

$$M_L = \frac{1 - p}{1 - \bar{\nu} p} \quad (\text{A6})$$

where p is the probability of a neutron to induce a fission in the item before leaking out, and $\bar{\nu}$ is the average number of neutron generated in fission. In this derivation parasitic absorption (capture) is neglected as is scattering (since the value of p implicitly embodies scattering). The equivalence is clear if we note that P_0 is the probability of no reaction, equivalent with $(1 - p)$ in (A6), whereas the ratio:

$$\frac{\sigma_s + \bar{\nu} \sigma_f}{\sigma_{tot}} \quad (\text{A7})$$

is the average number of secondaries per reaction.

An alternative way of putting it is that the case of capture, scattering and fission can be lumped together into a probability distribution of the number of secondaries per reaction by treating capture as a fission event with zero outcoming neutrons, and scattering as fission with one neutron produced. Then, the number distribution $p(k)$ of secondaries will be:

$$p(k) = \frac{\sigma_c}{\sigma_{tot}} \delta_{k,0} + \frac{\sigma_s}{\sigma_{tot}} \delta_{k,1} + \frac{\sigma_f}{\sigma_{tot}} f(k) \quad (\text{A8})$$

Its generating function $q_r(z)$ is given as:

$$q_r(z) = \frac{\sigma_c}{\sigma_{tot}} + \frac{\sigma_s}{\sigma_{tot}} z + \frac{\sigma_f}{\sigma_{tot}} q_f(z) \quad (\text{A9})$$

With this definition, Eq. (A3) can be written in the shorter form:

$$g(z) = P_0 z + (1 - P_0) q_r[g(z)] \quad (\text{A10})$$

It is easy to see that (A10) yields the same result for M_L as (A5). From (A10), the higher order factorial moments of $g(z)$ (the factorial moments of the number of neutrons emitted from the item initiated by one source neutron (Favalli et al., 2015)) can also be derived. These moments will have the same form as the traditional point model equations, with the only difference that the factorial moments $\nu_{f,i}$ $i = 1, 2, 3$ of $f(k)$, which can be obtained from the $q_f(z)$ of (A2) by differentiating with respect to z , have to be replaced by the factorial moments $\nu_{r,i}$ of the $p(k)$ of (A8), which can be derived from the $q_r(z)$ of (A9). This shows that one has the relation:

$$\nu_{r,i} = \frac{\sigma_f}{\sigma_{tot}} \nu_{f,i} + \frac{\sigma_s}{\sigma_{tot}} \delta_{i,1} \quad (\text{A11})$$

Data availability

Data will be made available on request.

References

- Behrens, D.J., 1949. The effect of holes in a reacting material on the passage of neutrons. Proc. Phys. Soc. A62 (1949), 607–616.
- Bell, G.L., Glasstone, S., 1970. Nuclear Reactor Theory. Van Nostrand Reinhold Company, NY.

- Bierman, S.R., Clayton, E.D., 1969. Criticality of transuranium actinides – under moderated systems. *Trans. Am. Nucl. Soc.* 12, 887–888.
- Bohnel, K., 1978. Determination of plutonium in nuclear fuels using the neutron coincidence method, Kernforschungszentrum, Karlsruhe report KFK-2203. Available in English translation as UK Atomic Weapons Research Establishment, AWRE translation number 70(54/4252). ISBN-0-85518121-4 (March, 1978).
- Bohnel, K., 1985. The effect of multiplication on the quantitative determination of spontaneously fissioning isotopes by neutron correlation analysis. *Nucl. Sci. and Engin.* 90, 75–82.
- Carlvik, I., 1967a. Collision probabilities for finite cylinders and cuboids. *Nucl. Sci. and Engin.* 30, 150–151.
- Carlvik, I., 1967b. Collision probabilities for finite cylinders and cuboids. *Aktiebolaget Atomenergi Report AE-281*. Stockholm, Sweden.
- Case, K.M., Hoffman, F. de, Placzek, G., Carlson, B., Goldstein, M., 1953. *Introduction to the Theory of Diffusion: Volume 1*, Los Alamos Scientific Laboratory. US Government Printing Office, Washington, DC.
- Cashwell, E.D., Everett, C.J., 1959. *A Practical Manual on the Monte Carlo Method for Random Walk Problems*. Pergamon Press, N.Y.
- Castle, H., Ibsen, H., Sacher, G., Weinberg, A.M., 1943. The effect of fast fission on k, metallurgical project Chicago metallurgical laboratory report CP-644 (May, 1943).
- Creutz, E., Jupnik, H., Snyder, T., Wigner, E.P., 1955. Effect of geometry on resonance absorption of neutrons by uranium. *J. Appl. Phys.* 26, 271–275.
- Croft, S., 1990. The distribution of emergent flight path lengths from homogeneous spheres. *Nucl. Instrum. and Meths. Phys. Res.* A288, 589–592.
- Croft, S., Favalli, A., 2017. Incorporating delayed neutrons into the point-model equations routinely used for neutron coincidence counting in nuclear safeguards. *Ann. Nucl. Energy* 99, 36–39.
- Croft, S., Henzlova, D., 2013. Determining ^{252}Cf source strength by absolute passive neutron correlation counting. *Nucl. Instrum. and Meths. in Phys. Res.* A714, 5–12.
- Croft, S., Miller, K., Reed, B.C., 2011. An estimate of prompt critical mass of a fissile nuclide including capture within the point-model. *Proc. 33rd ESARDA Annual Meeting, Helia Conference Hotel, Budapest, Hungary*.
- Croft, S., Favalli, A., Hauck, D.K., Henzlova, D., Santi, P.A., 2012a. Feynman variance-to-mean in the context of passive neutron coincidence counting. *Nucl. Instrum. and Meths. Phys. Res.* A686, 136–144.
- Croft, S., Henzlova, D., Hauck, D.K., 2012b. Extraction of correlated count rates using various gate generation techniques: Part I Theory. *Nucl. Instrum. and Meths. Phys. Res.* A691, 152–158.
- Crossley, D., Firkin, S.J., Green, J.J.W., Lee, J.A., 1994. Preparation of Characterized Encapsulated Plutonium Alloy Foils for Use as Calibration Standards for Non-destructive Assay Techniques, vol. 2. International Atomic Energy Agency publication STI/Pub, pp. 595–599. Paper IAEA-SM-333/190P.
- Dirac, P.A.M., 1943. Approximate rate of neutron multiplication for a solid of arbitrary shape and uniform density: Part I General Theory. *British Department of Scientific and Aeronautical Research Report MS-D- 5*, 372–382.
- Dirac, P.A.M., Fuchs, K., Peierls, R., Preston, P., 1943. Approximate rate of neutron multiplication for a solid of arbitrary shape and uniform density: Part II Application to the oblate spheroid, hemi-sphere and oblate hemi-spheroid. *British Department of Scientific and Aeronautical Research Report MS-D- 5*, 383–399.
- Ensslin, N., Harker, W.C., Krick, M.S., Langner, D.G., Pickrell, M.M., Stewart, J.E., 1998. *Application Guide to Neutron Multiplicity Counting*. Los Alamos National Laboratory Manual. LA-13422-M, November 1998.
- Favalli, A., Croft, S., Santi, P., 2015. Point model equations for neutron correlation counting: extension of Böhnel's equations to any order. *Nucl. Instrum. and Meths. Phys. Res.* A795, 370–375.
- Fleming, R.L., 1982. Neutron self-shielding factors for simple geometries. *Int. Journal Appl. Radiat. Isot.* 33, 1263–1268.
- García, R.D.M., 2004. Optimized algorithm for collision probability calculations in cubic geometry. *Nucl. Sci. and Engin.* 147, 148–157.
- Gavron, A., 1976. Angular distribution of neutrons from fission fragments. *Phys. Rev.* C13 (6), 2562–2563.
- Glasstone, S., Edlund, M.C., 1957. *The Elements of Nuclear Reactor Theory* (Sixth Printing). D. Van Nostrand Company, Inc., Princeton, N.J.
- Gorshkov, V.G., Tsvetkov, O.S., 1962. Distribution of paths of α -particles in a spherical source. *Soviet Phys. Tech. Phys.* 7, 565–566.
- Göttsche, M., Kirchner, G., 2015. Improving neutron multiplicity counting for the spatial dependence of multiplication: results for spherical plutonium samples. *Nucl. Instrum. and Meths. Phys. Res.* A798, 99–106.
- Gubbins, M.E., 1964. A Monte Carlo computer programme CEP for calculating collision probabilities in cuboids and finite cylinders, United Kingdom Atomic Energy Establishment Winfrith report AEEW-M442(March, 1964).
- Henzlova, D., Croft, S., Menlove, H.O., Swinhoe, M.T., 2012. Extraction of correlated count rates using various gate generation techniques: Part II Experiment. *Nucl. Instrum. and Meths. in Phys. Res.* A691, 159–167.
- Hsue, S.-T., Stewart, J.E., Sampson, T.E., Butler, G., Rudy, C.R., Rinard, P.M., 1997. *Guide to Nondestructive Assay Standards: Preparation Criteria, Availability, and Practical Considerations*. Los Alamos National Laboratory report LA-13340-MS (October, 1997).
- Huges, D.J., 1953. *Pile Neutron Research*. Addison-Wesley Publishing Company, Inc., Cambridge, Mass.
- Landers, N.F., Petrie, L.M., Bucholz, J.A., 1998. The material information processor for SCALE. Oak Ridge National Laboratory report ORNL/NUREG/CSD-2/R6(1998). Also known as NUREG/CR-0200.
- Langsdorf, A., Lane Jr., R.O., Monahan, J.E., 1956. Neutron Scattering angular distribution. Argonne National Laboratory report ANL-5567(June, 1956). The University of North Texas Digital Library: <http://digital.library.unt.edu/ark:/67531/metadc11511/>. (Accessed 9 April 2013).
- Langsdorf, A., Lane, Jr.R.O., Monahan, J.E., 1957. Angular distributions of scattered neutrons. *Phys. Rev.* 107 (4), 1077–1087.
- Larsen, W., 1980. On the chord length across a system, *Transport Theory and Statistical Physics* 1, 37–41.
- Liang, C., Ji, W., 2011. Chord length sampling in stochastic media packed with poly-sized spheres. *Trans. ANS* 104 (1), 331–333.
- Lindstrom, R.M., Fleming, R.L., 2008. Neutron self-shielding factors for simple geometries, revisited. *Chem. Anal. (Warsaw)* 53, 855–859.
- Littler, D.J., Raffle, J.F., 1957. *An Introduction to Reactor Physics*, second ed. Pergamon Press, London.
- Lovchikova, G.N., 1962. Scattering of fast neutrons on nuclei. *Sov. Atom. Energy* 13 (1), 648–649. Translated from *Atomnaya Énergiya* 13(1)(1962)60-61.
- Magurno, B.A., Kinsey, R.R., Scheffel, F.M., 1982. Guidebook for the ENDF/B-V nuclear data files. *Topical Report ENDF-328* (July, 1982) Brookhaven National Laboratory report BNL-NCS-31451.
- Maslov, V.M., Obložinsky, P., Herman, M., 2008. Review and assessment of nuclear cross section and nubar covariances for advanced reactor systems. Brookhaven National Laboratory report BNL-81884-2008-IR.
- Mazzolo, A., Roesslinger, B., 2003. Properties of chord length distributions of nonconvex bodies. *J. Math. Phys.* 44 (No.12), 6195–6208.
- Mazzolo, A., Roesslinger, B., Diop, C.M., 2003. On the properties of the chord length distribution, from integral geometry to reactor physics. *Ann. Nucl. Energy* 30, 1391–1400.
- McLeod, R.L., 1963. On the capture probability of radiation in a finite rod. United Kingdom Atomic Energy Authority, Reactor Group, Dounreay, Caithness, Scotland, TRG-Report 573(D), 16pp.
- Pál, L., Pázsit, I., 2009. The fast fission factor revisited. *Nucl. Sci. Engin.* 161, 111–118.
- Pashkin, Yu.G., 1970. Accuracy of the wigner approximation. *At. Energ.* 28 (2), 147–148.
- Pázsit, I., Dykin, V., 2022. Transport calculations of the multiplicity moments for cylinders. *Nucl. Sci. Engin.* 196 (2022), 235–249.
- Pázsit, I., Pal, L., 2007. *Neutron Fluctuations: A Treatise on the Physics of Branching Processes*. Elsevier (October 2007).
- Pázsit, I., Enqvist, A., Pál, L., 2009. A note on the multiplicity expressions in nuclear safeguards. *Nucl. Instrum. and Meths. Phys. Res.* A603, 541–544.
- Pázsit, I., Dykin, V., Darby, F., 2023. Space-dependent calculation of the multiplicity moments for shells with the inclusion of scattering. *Nucl. Sci. Engin.* (2023). <https://doi.org/10.1080/00295639.2023.2178249>.
- Pearlstein, S., 1996. Critical mass variation of ^{239}Pu with water dilution. *Nucl. Technol.* 113, 110–111.
- Sanchez, R., 1997. Critical mass of ^{237}Np . *Trans. ANS* 77, 243–244.
- Sauer, A., 1963. Approximate escape probabilities. *Nucl. Sci. and Engin.* 16, 329–335.
- U.S. DOE, 1997. *Nonproliferation and Arms Control Assessment of Weapons-Useable Fissile Material Storage and Excess Plutonium Disposition Alternatives*. The United States Department of Energy's Office of Arms Control and Nonproliferation report DOE/NN-007 (Jan).
- Walker, J., Weaver, D.R., 1979. Nuclear physics data for reactor kinematics. *Adv. Nucl. Sci. Technol.* 11, 1–66.
- Weinberg, A.M., Wigner, E.P., 1958. *The Physical Theory of Neutron Chain Reactors*. The University of Chicago Press.
- Wigner, E.P., Creutz, E., Jupnik, H., Snyder, T., 1955. Resonance absorption of neutrons by spheres. *J. Appl. Phys.* 26, 260–270. Errata *J. Appl. Phys.* 27(195)839.
- Wilson, R.R., 1947. Directional properties of fission neutrons. *Phys. Rev.* 72 (3), 189–192.
- Wright, R.Q., Jordan, W.C., Westfall, R.M., 2000. Critical masses of bare metal spheres using SCALE/XSDRN. *Trans. ANS* 82, 167–168.